Quantitative Proteomics Using Stable Isotope Labeling with Amino Acids in Cell Culture Reveals Protein and Pathway Regulation in Porcine Circovirus Type 2 Infected PK-15 Cells

Huiying Fan,[†,‡,§] Yu Ye,[†,‡,§] Yongwen Luo,[†,‡,§] Tiezhu Tong,[∥] Guangrong Yan,[⊥] and Ming Liao*[,†,‡]

[†]MOA Key Laboratory for Animal Vaccine Development, Guangzhou 510642, China

[‡]College of Veterinary Medicine, South China Agricultural University, Guangzhou 510642, China

[∥]Huizhou Entry-Exit Inspection and Quarantine Bureau, Huizhou 516001, China

[⊥]Institute of Life and Health Engineering and National Engineering and Research Center for Genetic Medicine, Jinan University, Guangzhou 510632, China

Ⓢ *Supporting Information*

ABSTRACT: The infection of host cells by porcine circovirus type 2 (PCV2) leads to extensive modulation of the gene expression levels of target cells. To uncover the pathogenesis and virus-host interactions of PCV2, a quantitative proteomic study using the stable isotope labeling with amino acids in cell culture (SILAC), coupled with mass spectrometry, was performed on PCV2-infected PK-15 cells. The SILAC-based approach identified 1341 proteins, 163 of which showed significant change in level at 72 h after infection (79 up-regulated and 84 down-regulated). The modulated proteins included a number of proteins involved in substrate transport, cytoskeletal changes, and the stress response. Changes in the expression levels of selected proteins were verified by Western blot analysis. Ingenuity Pathway Analysis was used to reveal protein and interactive pathway regulation in response to PCV2 infection. Functional network and pathway analyses could provide insights into the complexity and dynamics of virus—host cell interactions and may accelerate our understanding of the mechanisms of PCV2 infection.

KEYWORDS: porcine circovirus type 2, quantitative proteomics, stable isotope labeling with amino acids in cell culture (SILAC), pathway analysis
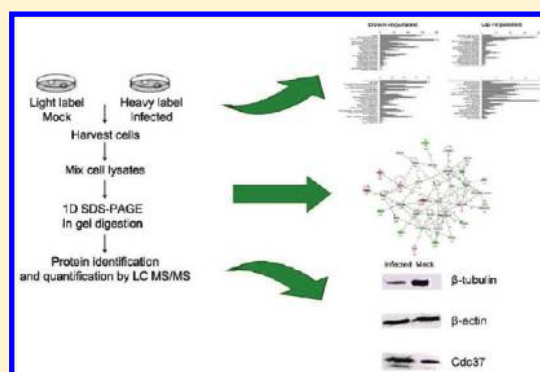
INTRODUCTION

Porcine circovirus type 2 (PCV2) is the primary etiological agent of porcine circovirus disease (PCVD). PCVD is an emerging disease that has been reported around the world for more than 10 years. It is characterized by weight loss, respiratory or digestive disorders and enlarged lymph nodes, with lymphocyte depletion, enteritis, pneumonia, vasculitis, ischemic lesions, reproductive failure and necrotizing dermatitis.[1−4] The pathogen, a member of the Circoviridae family and Circovirus genus, is a small, nonenveloped, single-stranded DNA virus.[5] The PCV virion is composed of coat protein subunits assembled into 12 pentameric units,[6] and the 1.7-kb viral genome contains 11 main open reading frames (ORFs), 3 of which have been characterized.[7] ORF1 encodes replicases (Rep), which are responsible for virus replication.[8] ORF2 encodes the immunogenic capsid (Cap), or coat protein, which assembles the viral capsid.[9] At least 3 conformational neutralizing epitopes within Cap have been identified, and this protein is involved in the development of cell-mediated immunity upon PCV2 infection.[10] A newly characterized protein, encoded by ORF3, has been reported as a nonstructural protein that is not

essential for PCV2 replication in cultured PK-15 cells but contributes to the virus-induced apoptosis of host cells by activating the initiator caspase-8 and effector caspase-3 pathways.[11] ORFs 4−11 of PCV2 have been identified, but the functions of the putative proteins that they encode are unknown.

Although PCVD causes substantial economic losses, PCV2 pathogenesis is not fully understood. PCV2 DNA influences cytoskeletal rearrangements in plasmacytoid and monocyte-derived dendritic cells, impairing the activation of these cells by certain viruses or Toll-like receptor ligands, which is associated with the secretion of α-interferon (α-IFN) and IL-12.[12] Meanwhile, with PCV2-associated disease, the increased expression levels of proinflammatory cytokines in target tissues and cells may play important roles in the immunopathological response.[13,14] A portion of the genome of PCV2, made up of oligodeoxynucleotides (ODNs) with central CpG motifs, has an inhibitory effect on the production of α-IFN in porcine peripheral blood mononuclear cells.[15] To date, little is known

regarding the mechanisms underlying the pathogenesis and immunosuppression of PCV2-induced diseases and the viral interactions with the host immune system.

A better understanding of the interaction between host cells and PCV2 could lead to an increased understanding of the alterations induced by viruses with respect to energy metabolism and signal transduction. A number of cellular pathways are known to change in PCV2-infected cells in culture and in vivo. PCV2 ORF3 protein competes with p53 for binding to Pirh2 and mediates the deregulation of p53 homeostasis, leading to increased p53 levels and apoptosis of infected cells.[16] The JNK1/2 and p38 MAPK pathways are activated in PCV2-infected PK-15 cells, and inhibition of these pathways results in significant reductions in PCV2 viral mRNA transcription and protein synthesis, viral progeny release, and blockage of PCV2-induced apoptotic caspase-3 activation.[17] The Cap and Rep proteins interact with cytoskeletal proteins and other proteins, including hsp40, during the course of the viral life cycle.[18−20] In addition, it is unclear how PCV2 modulates the expression and modification of host cells for its replicative advantage or why PCV2 causes a multisystemic disorder in weaned piglets.

We utilized a modern, quantitative proteomics approach to further analyze the proteomic changes caused by PCV2 replication. Several recent studies have been conducted using this approach, including those investigating influenza A virus,[21] severe acute respiratory syndrome (SARS)-associated corona-virus,[22] pseudorabies virus,[23] infectious bronchitis virus,[24] adenovirus,[25] hepatitis C virus,[26] human respiratory syncytial virus[27] and human immunodeficiency virus (HIV).[28] The use of quantitative mass spectrometry (MS) coupled with stable isotope labeling by amino acids in cell culture (SILAC) to compare uninfected and infected cells is more accurate than traditional two-dimensional gel electrophoresis for quantifying low-abundance proteins. Here, we report the quantitative whole-cell proteome analysis of PCV2 infection, in which alterations of PK-15 cells were characterized by quantitative MS/SILAC. In total, 163 proteins whose abundance was significant altered (significance B ≤ 0.05) were identified, including heat shock proteins, proteins involved in cellular growth and proliferation, and proteins associated with cellular metabolism and substrate transport. Most importantly, several proteins that are involved in the modulation of system-level dysfunction were identified, which may provide a greater understanding of why piglets display multiform clinical syndromes following PCV2 infection.

■ MATERIALS AND METHODS

Virus and Cells

PK-15 cells were provided by the Collection of Cell Lines in the College of Veterinary Medicine, South China Agricultural University, China. PCV2 virus, which was isolated from a pig farm in the Guangdong Province of China, was propagated on a PK-15 cell monolayer.

Stable Isotope Labeling

Dulbecco's Modified Eagle's Medium was supplemented with 10% dialyzed fetal calf serum and all missing amino acids (Pierce) except L-lysine. The medium was then divided and supplemented with $^{12}C_6$ L-Lysine-2HCl or $^{13}C_6$ L-Lysine-2HCl (Pierce) to produce light or heavy SILAC medium, respectively. PK-15 cells were grown in parallel in both media, and passaging was routinely performed every 2−3 days (as appropriate) at

80−90% confluence. After at least five cell doublings, the cells had achieved almost complete incorporation of heavy L-lysine.

Infection

Cells that were cultured in a conventional source of amino acids were used as mock-infected controls, while heavy-labeled cells were infected with PCV2. Cell batches that were passaged in the two media were seeded in 75-cm² cell culture flasks until they reached 75% confluence. They were then inoculated with virus stock corresponding to a multiplicity of infection (MOI) of 1 (heavy-labeled cells) or were mock inoculated (light-labeled cells). The amount of dialyzed serum in the SILAC media was decreased to 2%. The PK-15 cells were harvested at 72 h postinfection (h p.i.).

Preparation of Protein Samples and In-gel Trypsin Digestion

Cell pellets were resuspended in a cold lysis buffer and incubated for 10 min on ice. The lysate was sonicated for ten cycles of 0.8 s on and 0.8 s off and centrifuged to pellet the cellular debris. Protein quantification was measured using the Bradford protein assay with 2-D Quant Kit (PlusOne). Prior to gel electrophoresis, equal amounts of PCV2-infected cells and uninfected cells proteins were mixed, separated using 10% SDS-PAGE, and silver stained to visualize the gel bands.The gel lanes were cut horizontally into gel pieces that were then in-gel destained, reduced, alkylated and digested with gold-trypsin at 37 °C overnight as described previously, respectively.[25,29] The tryptic peptides were extracted, and the peptide mixtures were concentrated by SpeedVac centrifuge to dryness and redissolved with 2% acetonitrile (ACN) in 0.1% formic acid before LC−MS/MS analysis.

■ LC−MS/MS ANALYSIS

The peptide mixtures were separated by HPLC (Agilent 1200) on a C18 reverse phase column, and analyzed using an LTQ-Orbitrap mass spectrometer (Thermo Electron). The spray voltage was set to 1.85 kV, and the temperature of the heated capillary was set to 200 °C. Full scan MS survey spectra (m/z 400−2000) in profile mode were acquired in the Orbitrap with a resolution of 60000 at m/z 400 after the accumulation of 1000000 ions. The five most intense peptide ions from the preview scan in the Orbitrap were fragmented by collision-induced dissociation (normalized collision energy 35%, activation Q 0.25 and activation time 30 ms) in the LTQ after the accumulation of 5000 ions. Precursor ion charge state screening was enabled, and all unassigned charge states and singly charged species were rejected. The dynamic exclusion list was restricted to a maximum of 500 entries with a maximum retention period of 90 s and a relative mass window of 10 ppm. The data were acquired using Xcalibur software (Thermo Electron).

■ PROTEIN IDENTIFICATION, QUANTIFICATION AND BIOINFORMATICS

Protein identification and quantitation were performed as previously described with minor modifications.[30] In brief, raw MS spectra were processed by using MaxQuant 1.0.13.13 software and the derived peak lists were searched using the Mascot 2.2.04 search engine (Matrix Science, London, U.K.) against a concatenated forward-reverse database from the National Center for Biotechnology information nonredundant (NCBinr) database (July 20, 2010) containing pig (*sus scrofa*)
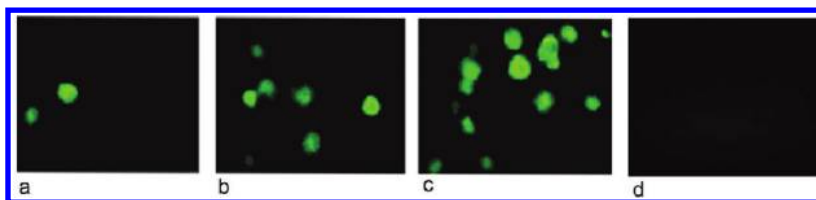
Figure 1. Dynamics of PCV2 growth by IFA staining in infected PK-15 cells at (a) 24, (b) 48 and (c) 72 h p.i. and (d) mock-infected cells at 72 h, shown as a control. Images were taken at an original magnification of 200×.

sequences. The following search parameters were employed: full tryptic specificity was required, two missed cleavages were allowed; Carbamidomethylation was set as fixed modification, whereas either "light" (Lys0)- or "heavy" (Lys6)-lysine and Oxidation (M) were considered as variable modifications. Precursor ion mass tolerances were 10 ppm for all MS acquired in the Orbitrap mass analyzer, fragment ion mass tolerance was 0.5 Da for all MS2 spectra acquired in the LTQ. Mascot search results were further processed by the MaxQuant 1.0.13.13 at the FDR 1% at both the protein, peptide and site level. The normalized H/L ratios, significance and variability(%) were automatically produced by MaxQuant 1.0.13.13 programm. The resulting proteingroups.txt output file from MaxQuant containing the peptide identifications was imported into Microsoft Excel, in which additional filtering was performed (protein posterior error probability (PEP) ≤0.01). Gi numbers of all significantly regulated proteins and some unaltered proteins were imported into the Ingenuity Pathway Analysis software (IPA, www.ingenuity.com) for bioinformatics analysis based on published reports and databases such as Gene Ontology, Uniport and TrEMBL.

Western Blot Analysis

The protein concentrations of PCV2-infected and uninfected cell lysates, harvested at 72 h p.i., were measured. Equivalent amounts of cell lysates from two independent biological replicates were denatured in 5× sample loading buffer by heating at 70 °C for 10 min and were then separated by 10% SDS-PAGE. Proteins were electrotransferred to 0.45-μm nitrocellulose membranes (Bio-Rad). Membranes were blocked with 5% nonfat dry milk in TBS containing 0.05% Tween-20 (TBST) overnight at 4 °C and then incubated for 1 h at room temperature with rabbit polyclonal antibodies against Cdc37 (Bioworlde Technology, Inc.), β-tubulin (Bioworlde Technology, Inc.) or β-actin (Bioworlde Technology, Inc.). Membranes were washed in TBST and incubated with DyLight488-conjugated goat antirabbit IgG (1:10000, Rockland) for 1 h. Membranes were washed in TBST and visualized using the Odyssey Infrared Imaging system (Licor Biosciences, Lincoln, NE).

Immunofluorescence Assay (IFA)

Infected cells were washed with PBS, fixed with cold acetone/ethanol (3/2) at −20 °C for 30 min and washed again with PBS. The cells were then incubated with pig anti-PCV2 hyperimmune serum at 37 °C for 1 h, washed four times with PBST (0.05% Tween-20 in PBS, pH 7.4), and further incubated with rabbit antipig IgG conjugated to FITC (Sigma) at 37 °C for 1 h in the dark. After four washes with PBST, the numbers of infected cells were quantified by fluorescence microscopy.

RESULTS

Confirmation of PCV2 Infection in PK-15 Cells

Because PCV2 does not induce a typical cobblestone morphology in PK-15 cells, viral infection was confirmed by the detection of PCV2 antigen using IFA at 24, 48, and 72 h p.i., performed as described previously for the classical swine fever virus (CSFV).[31] Mock-infected cells were grown in medium containing light L-lysine, and virus-infected cells were grown in medium containing heavy L-lysine. The results clearly showed green fluorescence in PCV2-infected PK-15 cells, while the mock-infected cells showed no fluorescence. Quantitative proteomic analysis, used to investigate the potential changes to the host cell proteome during PCV2 infection and replication, required a high proportion of PCV2-infected PK-15 cells. Active viral replication was well underway in virtually all of the examined cells. Fluorescence microscopy indicated that PCV2 titers increased during the first 24 h of infection and that 60−70% of cells that were treated with PCV2 were infected at 72 h p.i. (Figure 1). PK-15 cells at 72 h p.i. were therefore selected for proteomic analysis, in accordance with a study by Xin Zhang.[20]

SILAC analyses of the proteomes of virus-infected cells. No previous study has used SILAC coupled with LC−MS/MS to identify and quantify the proteomic changes that occur in PCV2-infected cells. In this study, we obtained cellular proteomes from PCV2-infected and mock-infected PK-15 cells and compared the differences in the levels of the isolated proteins by quantitative proteomics.

Labeled PK-15 cells were infected with PCV2 at MOI 1 or mock-infected with supernatant that was prepared as described for the labeled virus stock. Our research strategy is summarized in Figure 2.
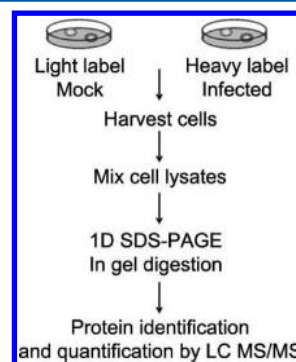
Figure 2. Experimental strategy of SILAC coupled with LC−MS/MS.

Here, total 7726 peptides and 1341 proteins were detected, 4536 (58.71%) peptides and 1054 (78.60%) proteins could be quantified, respectively. Of these, 84 proteins were highly down-regulated, and 79 were significantly up-regulated at a significance B value ≤0.05 as calculated by MaxQuant[30]

(Figure 3 and Table 1); 1178 proteins (87.84%) did not significantly change in abundance or could not be quantified with respect to protein abundance.
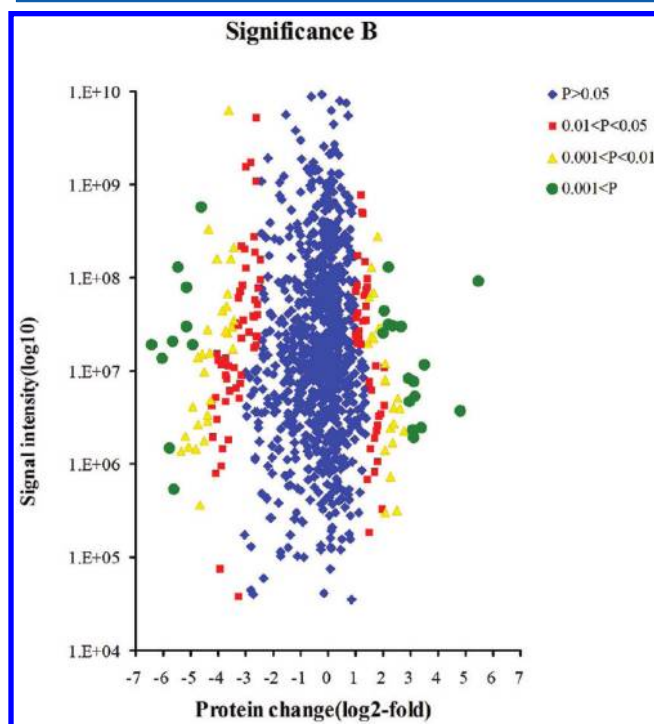
Figure 3. Proteome-wide accurate quantitation and significance. Signal intensities($\log_{10}$) of all quantified proteins in the PCV2 infected experiment are shown as a function of their fold change($\log_2$). The spread of the cloud is lower at high abundance, indicating that quantification is more precise. The criteria as being identified as a significantly regulated protein can be evaluated by the significance B level indicated in blue, red, yellow and green, respectively.

Subcellular and Functional Characterization of Identified Proteins and Bioinformatics Analysis

To gain functional insights into the cellular proteome, the 163 identified proteins were assigned to different molecular functional classes and subcellular annotations based on the underlying biology evidence from the UniProtKB/Swiss-Prot and TrEMBL protein databases and the Gene Ontology database.

We examined the localizations of the 163 identified proteins. The up-regulated proteins (Figure 4A) in infected cells were localized to the cytoplasm (32.91%), cytoplasm and nucleus (22.78%), nucleus (13.92%), membrane (11.39%), mitochondrion (6.33%), membrane and cytoplasm (6.33%), cytoskeleton (3.8%), mitochondrion and nucleus (1.27%) and ribosome (1.27%). Down-regulated proteins (Figure 4B) were localized to the cytoplasm (23.81%), nucleus (19.05%), cytoplasm and nucleus (14.29%), mitochondrion (13.10%), ribosome (9.52%), cytoskeleton (7.14%), unknown cellular location (4.76%), membrane (3.57%), membrane and cytoplasm (1.19%), cytoplasm and mitochondrion (1.19%), membrane and mitochondrion (1.19%), and nucleus and ribosome (1.19%).

Because the pig genome database had poor annotation compared to the human genome and because many proteins were unassigned or uncharacterized, gene identifications of the identified proteins in Table 1 were converted to human protein gi numbers. Protein gi numbers and levels of regulation were imported into the Ingenuity Pathways Analysis (IPA) tool, and interacting pathways were constructed based on the underlying biological evidence from the literature database.

Organizing the previously characterized 163 proteins into distinctive functional groups reveals that the proteome differed between increases and decreases, which gave a variety of meaningful information. Diseases and disorders, molecular and cellular functions, physiological system development and functions and toxicity functions that were identified at statistically significant levels ($p \leq 0.05$) are depicted in Figure 5, with additional data shown in Supplementary Table 2 (Supporting Information).

The 79 up-regulated proteins, which correspond to 24 diseases and disorders (Figure 5A, right), included proteins that are related to genetic disorder, neurological disease, cancer, developmental disorder, skeletal and muscular disorders, and reproductive system disease. These up-regulated proteins can also be assigned to 30 molecular and cellular functions groups (Figure 5B, right), including small molecule biochemistry, cellular growth and proliferation, lipid metabolism, molecular transport, cellular function and maintenance, cellular assembly and organization, and cell death; 22 physiological system development and functions groups (Figure 5C, right), including tissue development, embryonic development, organismal development, connective tissue development and function, and nervous system development and function; and 7 toxicity functions groups (Figure 5D, right), including liver hepatitis, liver cholestasis, renal hypertrophy, and nephrosis. 84 other proteins, which are primarily involved in 23 diseases and disorders (Figure 5A, left), including a genetic disorder, cancer, reproductive system disease, skeletal and muscular disorders, and immunological disease. These down-regulated proteins are also assigned to 28 molecular and cellular functions groups (Figure 5B, left), including cell death, cellular assembly and organization, cellular function and maintenance, cell morphology, protein synthesis, cellular growth and proliferation, and small molecule biochemistry; 24 physiological system development and functions groups (Figure 5C, left), including cardiovascular system development and function, tissue development, tissue morphology, and connective tissue development and function; and 5 toxicity functions groups (Figure 5D, left), including cardiac necrosis/cell death, liver necrosis/cell death, cardiac damage, liver cholestasis, and cardiac regeneration.

Proteins that changed significantly in virus-infected cells were mapped to 10 specific functional networks (Figure 6), with each network containing 11 or more "focus" members (Supplementary Table 2, Supporting Information). The four networks of interest correspond to (1) cellular movement, cellular assembly and organization, cell-to-cell signaling and interaction (Figure 7A); (2) cellular assembly and organization, cellular function and maintenance, energy production (Figure 7B); (3) cell death, hematological system development and function, cellular development (Figure 7C); (4) gene expression, cell cycle, protein synthesis (Figure 7D). Proteins that are present in these pathways and identified in our analysis as up-regulated are depicted in shades of red, and those that were identified as down-regulated are shown in green. Proteins known to be in the network but were not identified in our study are depicted in white.

Validation of Protein Identification and Quantification

To confirm the protein quantification, three proteins with altered abundances (β-tubulin, Cdc37 and β-actin) for which antibodies were available were chosen to rigorously validate the identification and SILAC results. As shown in Figure 8, the

Table 1. Proteins Regulated Significantly (B ≤ 0.05) in PCV2-infected versus Mock-Infected PK-15 Cells, as Identified by LC−MS/MS[a]

protein name	accession number	ratios (infection/ control)	peptides	functions
		Proteins present in increased abundance in PCV2-infected cells		
Similar to GTP cyclohydrolase I feedback regulator	gi|194034891	5.7091	3	Mediates tetrahydrobiopterin inhibition of GTP cyclohydrolase 1
Similar to Serine hydroxylmethyltrans ferase 2	gi|194037572	4.6143	12	Interconversion of serine and glycine
Cystathionine gamma-lyase	gi|113205776	3.8388	4	Cystathionine gamma-lyase activity
Asparagine synthetase	gi|262036930	3.4583	16	Asparagine synthase (glutamine-hydrolyzing)
Spermidine synthase	gi|45359357	2.984	2	Catalytic activity
Similar to myasthenia gravis autoantigen gravin	gi|194033447	11.215	2	Mediates the subcellular compartmentation of protein kinase A (PKA) and protein kinase C (PKC)
Hypothetical protein	gi|194040747	10.39	3	Unknown
Similar to GalNAc kinase	gi|194034756	4.1638	1	Acts on GalNAc
Dihydrolipoamide acetyltransferase	gi|14587786	2.0339	11	Dihydrolipoyllysine-residue acetyltransferase
Hexosaminidase B (beta polypeptide)	gi|262072808	2.0166	6	Beta-N-acetylhexosaminidase activity
Developmentally regulated GTP binding protein 1 isoform 2	gi|194043276	4.0931	8	Cell proliferation, differentiation and death
SWI/SNF related, matrix associated, actin dependent regulator of chromatin, subfamily b, member 1	gi|194043360	2.9353	2	Cell proliferation and differentiation, cellular antiviral activities and inhibition of tumor formation
Spermatid perinuclear RNA binding protein	gi|194033567	2.8574	1	Regulation of cell growth
Platelet-activating factor acetyl hydrolase Ib-alpha subunit	gi|11276042	2.0938	13	Positively regulates the activity of dynein
NCK-associated protein 1 isoform 2	gi|194043983	3.1118	6	Controls Rac-dependent actin remodeling,apoptosis
Similar to CG3552 CG3552-PA	gi|194039676	3.5318	3	Unknown
Ribonucleotide reductase M2	gi|262263187	8.4174	2	Ribonucleoside-diphosphate reductase activity
Similar to DNA Primase polypeptide 2	gi|194040260	6.8085	2	Synthesizes small RNA primers
NCK adaptor protein 1	gi|208612652	3.6289	1	Plays a role in the DNA damage response
Similar to telomerase-associated protein 1	gi|194038982	43.495	3	Component of the telomerase ribonucleoprotein complex
UDP-N-acteylglucosamine pyrophosphorylase 1	gi|194036852	3.8094	4	UDP-N-acetylglucosamine diphosphorylase activity
B56, delta isoform	gi|147223351	3.2706	2	Protein phosphatase type 2A regulator activity
6-Phosphofructo-2-kinase/fructose-2,6-biphosphatase 1	gi|217314909	3.2103	2	6-phosphofructo-2-kinase activity
Similar to Putative hexokinase HKDC1	gi|194042318	2.8426	5	Hexokinase
Serine/threonine-proteins phosphatase 2A 55 kDa regulatory subunit B alpha isoform	gi|255683519	2.1297	6	Modulates substrate selectivity and catalytic activit
Similar to rho/rac guanine nucleotide exchange factor 2	gi|194036037	8.6784	4	Activates Rho-GTPases
Delta(3,5)-Delta(2,4)-dienoyl-CoA isomerase	gi|113205878	4.2112	2	Catalytic activity
Acetyl-CoA carboxylase alpha	gi|159895418	3.8458	6	Involved in the biogenesis of long-chain fatty acids
CDP-diacylglycerol–inositol 3-phosphatidyl transferase	gi|262072933	3.5223	2	Catalyzes the biosynthesis of phosphatidylinositol
Peroxisomal multifunctional enzyme type 2	gi|47523670	2.6399	20	Oxidoreductase activity
Similar to uracil phosphoribosyl ransferase (FUR1) homologue	gi|194045009	4.1069	1	Nucleoside metabolic process
Similar to cytosolic IMP-GMP speci fic 5-nucleotidase	gi|194041955	2.0428	7	Nucleotidase
Thioredoxin reductase 1, cytoplasmic	gi|255918208	4.0975	2	Glutaredoxin activity and thioredoxin reductase activity
NAD(P)H dehydrogenase[quinone]1	gi|227430403	2.6931	6	Quinine reductase
Aldo-keto reductase	gi|158148957	2.5097	13	Oxidoreductase activity
NADP dependent leukotriene b4 12- hydroxyde hydrogenase	gi|1100737	2.3021	15	2-alkenal reductase activity
Apoliprotein A-I binding protein	gi|110832720	2.6183	4	Binding activity
Cytochrome P450, family51, subfamily A, polypeptide 1	gi|262072941	2.0172	7	Monooxygenase activity
Calcium-activated neutral proteinase 1 (calpain 1)	gi|19883961	28.298	3	Calcium-regulated nonlysosomal thiol-protease
Calcium-dependent protease small subunit	gi|115613	2.4657	10	Cytoskeletal remodeling and signal transduction
GalNAc-T2	gi|194042623	5.1066	3	Involved in O-linked oligosaccharide biosynthesis
Similar to FK506 -bindingprotein 5	gi|194040378	2.6372	5	Peptidyl-prolyl cis−trans isomerase activity
Hsp90 cochaperone Cdc37	gi|178057067	2.113	6	promotes kinases interaction with Hsp90 complex
Ribosomal protein S4	gi|194044996	6.2681	8	rRNA binding structural constituent of ribosome
DEAD box polypeptide 58	gi|224176124	7.8728	3	ATP-dependent helicase activity
Similar to DEAD box polypeptide 18	gi|194043658	3.3177	8	Probable RNA-dependent helicase
Similar to DEAD (Asp-Glu-Ala-Asp) box polypeptide 55	gi|194042858	2.9839	4	ATP-dependent helicase activity
Similar to cleavage and poly adenylation specific factor 6, 68 kD	gi|194037734	8.8021	2	Post-transcriptional gene expression processes
Similar to RNA-binding protein 8A	gi|194036316	2.8441	2	Component of exon junction complex
Similar to TRM5 tRNA methyl transferase 5 homologue (S. cerevisiae)	gi|194034229	2.6758	2	tRNA processing
Similar to programmed cell death 11	gi|194041963	2.2698	7	The generation of mature 18S rRNA

Table 1. continued

protein name	accession number	ratios (infection/ control)	peptides	functions
Proteins present in increased abundance in PCV2-infected cells				
Dyskeratosis congenita 1	gil213688833	2.1355	4	Pseudouridine synthase activity
Similar to Basic leucine zipper and W2 domain-containing protein 1	gil194043746	5.1172	7	Enhances histone H4 gene transcription
Zinc finger homeobox 4	gil194037155	3.9813	4	Cell differentiation,transcriptional regulation
Similar to TATA-binding protein- associated factor 172	gil194042483	3.0066	2	Regulates transcription
Interferon regulatory factor 6	gil17225490	2.7332	3	Sequence-specific DNA binding transcription
Neurofilament light polypeptide	gil194041508	8.7526	2	Structural constituent of cytoskeleton
Similar to NADH-coenzyme Q reductase	gil194036880	5.2002	10	Transfer of electrons from NADH to the respiratory chain
Calcineurin catalytic subunit delta isoform	gil14209665	4.1972	3	Phosphoprotein phosphatase activity
Methylmalonyl-CoA mutase	gil22293509	4.1784	4	Methylmalonyl-CoA mutase activity
Fructose-bisphosphate aldolase A	gil38230151	2.3392	4	Glycolysis
MHC class I antigen	gil168828737	4.8153	5	MHC class I protein complex
Caveolin 1	gil110962347	2.8061	3	T cell costimulation
Similar to nuclear receptor coactivator 5	gil194044705	3.406	2	ATP binding,aminoacyl-tRNA ligase activity
GNAS complex locus	gil147223307	4.2692	4	Signal transducer activity
Signal sequence receptor, alpha	gil297632426	2.167	3	Regulate the retention of ER resident proteins
Similar to UB fusion protein 1 homologue	gil194043450	3.6079	5	the ubiquitin-dependent proteolytic pathway
Proteasome 26S subunit, ATPase, 6	gil194034456	2.0027	7	ATP-dependent degradation of ubiquitinated proteins
Anaphase promoting complex subunit 5	gil194042928	4.876	1	Mediating ubiquitination and degradation of proteins
Karyopherin alpha 2	gil239923313	4.5147	5	Protein transporter activity
RAB5A	gil115394760	2.4284	4	The fusion of plasma membranes and early endosomes
Similar to very low density lipoprotein receptor				
VLDL-R2	gil194034163	2.1476	5	Receptor activity
Solute carrier family 3 member 2, cd98	gil171465894	2.0995	16	Light chain amino-acid transporters
Bicaudal C homologue 1 (Drosophila)	gil194042678	6.15	2	Regulates Golgi-endoplasmic reticulum transport
Copine I	gil217314903	5.1532	8	Membrane trafficking
ATPase, H$^+$ transporting, lysosomal 42 kDa, V1 subunit C1	gil298104138	3.1447	8	Proton-transporting ATPase activity
Importin 5	gil194040685	2.4263	26	Functions in nuclear protein import
Ryanodine receptor 1	gil1173335	7.5845	4	Ryanodine-sensitive calcium-release channel
Similar to ATPase, Cu(2+)-transporting, beta poly-peptide	gil194040582	5.7964	1	Copper-exporting ATPase activity
Proteins present in decreased abundance in PCV2-infected cells				
Vimentin	gil76097691	0.16471	29	structural molecule activity
Gelsolin	gil121118	0.15415	13	actin filament polymerization
Vimentin	gil21431723	0.12397	15	structural molecule activity
Tropomyosin 3	gil45272586	0.08525	17	actin binding
Desmin	gil48374063	0.04760	4	structural molecule activity
Tubulin, alpha 4a	gil194043859	0.16172	19	Structural molecule activity
56 kDa actin-sequestering protein	gil246858	0.09159	1	Actin binding, cytoskeleton organization
Similar to Myosin-Ie (Myosin-Ic)	gil194035082	0.06331	2	Microfilament motor activity
SPTAN1	gil44890896	0.05197	3	Regulation of receptor binding and actin cross-linking
Similar to Kinesin-like protein KIF7	gil194039647	0.03583	1	Microtubule motor activity
Collagen	gil194043714	0.01515	1	Serine-type endopeptidase inhibitor activity
Cardiac muscle ATP synthase H$^+$ transporting mitochondrial F1 complex alpha subunit 1	gil187370717	0.18233	12	proton-transporting ATPase activity
Similar to ATP synthase subunit beta, mitochondrial	gil194037554	0.11197	22	Hydrogen-exporting ATPase activity
Fumarate hydratase	gil120604	0.06101	5	Fumarate hydratase activity
Electron-transfer-flavoprotein, alpha polypeptide	gil194039680	0.03321	4	Transferring the electrons to the respiratory chain
Signal transducer and activator of transcription 3	gil113205774	0.04193	7	Signal transducer activity,transcription activator activity
Solute carrier family 9 member 3 regulator 1	gil217031226	0.07469	5	Regulation of sodium:hydrogen antiporter activity
High mobility group protein 1	gil123371	0.18252	7	DNA bending activity
Helicase SKI2W	gil156120140	0.10274	1	ATP-dependent helicase activity
High mobility group protein 2	gil123375	0.09934	2	DNA bending activity
H2A histone family member Z	gil166407422	0.06835	3	Nucleosome assembly
Histone H1.2-like protein	gil68534962	0.03293	4	Nucleosome assembly
Similar to SCP-1, partial	gil194036417	0.09244	2	Nuclei assembly and chromosomal synapsis
Similar to minichromosome maintenance complex component 4	gil194036759	0.08121	5	DNA-dependent DNA replication initiation

Table 1. continued

protein name	accession number	ratios (infection/ control)	peptides	functions
		Proteins present in decreased abundance in PCV2-infected cells		
Similar to Histone H1.1	gil194039760	0.07837	5	Nucleosome assembly
Similar to Fanconi anemia, complementation group E	gil194040359	0.06686	2	Associated the FA complex with FANCD2
Similar to ankyrin repeat domain 26	gil194044182	0.02805	3	Phosphorylated upon DNA damage
Heat shock 10 kD protein	gil30525868	0.14923	2	Chaperone binding
Heat shock 60 kDa protein 1 (chaperonin) isoform 1	gil194044029	0.10849	15	ATP binding
Heat shock 105 kDa/110 kDa protein 1	gil141521428	0.08746	14	ATP binding
pDJA1 chaperone	gil30351104	0.05298	2	Heat shock protein binding
Heat shock 27 kDa protein	gil75062102	0.04128	11	Involved in stress resistance and actin organization
T-complex protein 1 subunit zeta	gil2501139	0.01997	3	Unfolded protein binding
Ubiquitin-specific peptidase 7	gil205363467	0.11599	21	Ubiquitin thiolesterase activity
Autophagy related 16-like protein 1 transcript variant 1	gil296874478	0.07439	1	Degradation of most long-lived proteins
Sperm associated antigen 1	gil165909668	0.03936	1	Binding GTP and has GTPase activity
Similar to Leucine-rich repeat protein SHOC-2	gil194042023	0.06964	2	Regulatory subunit of protein phosphatase
130 kDa regulatory subunit of myosin phosphatase	gil4579751gg	0.04452	1	Regulates myosin phosphatase activity
Splicing factor 3b, subunit 1, 155 kDa	gil194044035	0.1667	10	Nuclear mRNA splicing
PRP40 pre-mRNA processing factor 40 homologue A	gil194044124	0.15413	5	mRNA processing
Zinc finger CCCH-type containing 14	gil194038226	0.06112	2	Binding the polyadenosine RNA oligonucleotides
Similar to ElaC homologue 1 (*E. coli*)	gil194034996	0.03741	1	Some tRNA 3′-processing endonuclease activity
Alanyl-tRNA synthetase 2, mitochondrial (putative)	gil194039401	0.02051	1	Alanyl-tRNA synthetase activity
UMP-CMP kinase	gil1096714	0.11188	4	Phosphotransferase activity
Similar to phosphate cytidylyltransferase 1, choline, beta	gil194044828	0.02748	2	Choline-phosphate cytidylyltransferase actiivity
Similar to sorbitol dehydrogenase	gil194034819	0.16845	7	L-iditol 2-dehydrogenase activity
Fas-associating death domain-containing protein	gil46397561	0.05526	3	Acting caspase-8
DNA-directed RNA polymerase II polypeptide B	gil8489819	0.04805	2	DNA-directed RNA polymerase activity;
POU domain region; homologue of mouse brn-3	gil454293	0.04378	1	DNA binding transcription regulation
Topoisomersae II	gil2668414	0.02988	4	DNA topoisomerase (ATP-hydrolyzing) activity
Similar to PC4 and SFRS1-interacting protein	gil194034110	0.01179	2	Regulation of transcription
Similar to KAT protein	gil194036918	0.07857	4	Possible role in tumorgenesis
Kinesin family member 4A isoform 2	gil194045130	0.06015	1	Mitotic chromosomal positioning, spindle stabilization
Similar to Protein C14orf166	gil194034448	0.05904	4	Interaction between C14ORF166 and NIN
Lectin galactoside-binding soluble 12 protein	gil215254104	0.05107	1	Cell cycle regulation
Similar to KIAA0979 protein	gil194040532	0.03718	2	DNA binding
Similar to coiled-coil domain containing 109A	gil194042794	0.16525	4	Unknown
Kelch repeat and BTB (POZ) domain containing 6, partial	gil194040718	0.08348	1	Unknown
Similar to LOC528833 protein	gil194038849	0.06959	2	Unknown
Similar to Ezrin (p81) (Cytovillin) (Villin-2)	gil194033419	0.00679	14	Unknown
60S ribosomal protein L7a	gil6174957	0.16157	5	Structural constituent of ribosome
40S ribosomal protein S15	gil47523728	0.1579	3	Structural constituent of ribosome
40S ribosomal protein S3	gil113205854	0.12298	14	Structural constituent of ribosome
60S ribosomal protein L10	gil113205616	0.10922	3	Structural constituent of ribosome
60S ribosomal protein L18	gil3122678	0.10397	3	Structural constituent of ribosome
60S ribosomal protein L23	gil194018720	0.07962	2	Structural constituent of ribosome
60S ribosomal protein L12	gil45268981	0.07468	7	Structural constituent of ribosome
40S ribosomal protein S16	gil212549659	0.02834	1	Structural constituent of ribosome
Motile sperm domain containing 2	gil194044779	0.10632	2	Structural molecule activity
Similar to 40S ribosomal protein S10	gil194040330	0.08059	3	Translational elongation
ADP/ATP translocase 3	gil47523888	0.17095	10	Catalyzing the exchange of ADP and ATP
Solute carrier family 25 member 3	gil255964672	0.15955	8	Transmembrane transport
Chloride intracellular channel protein 1	gil52000924	0.15668	5	Voltage-gated chloride channel activity
Transitional endoplasmic reticulum ATPase	gil1174636	0.14374	42	transitional endoplasmic reticulum
Small calcium-binding mitochondrial carrier 1	gil186886352	0.09316	3	Calcium ion binding
SEC24 related gene family, member C (*S. cerevisiae*)	gil194042814	0.16678	14	ER to Golgi vesicle-mediated transport
Similar to guanine nucleotide-exchange protein	gil194036657	0.13411	4	Promoting the activation of ARF1/ARF3
Similar to mitochondrial citrate transport protein	gil194043438	0.11762	3	Tricarboxylate transport
Similar to ribosome receptor	gil194044286	0.1113	11	Integral to endoplasmic reticulum membrane
Similar to Golgin subfamily A member 4, partial	gil194040817	0.10488	2	Vesicle-mediated transport
Similar to BFA-resistant GEF 1	gil194041915	0.05898	3	Protein binding

Table 1. continued

protein name	accession number	ratios (infection/ control)	peptides	functions
		Proteins present in decreased abundance in PCV2-infected cells		
Sec1 family domain containing 1	gil194038813	0.04851	4	Involved in Golgi-to-ER retrograde transport
Annexin A1	gil20141168	0.00722	30	Calcium-dependent phospholipid binding
Transporter 2, ATP-binding cassette, subfamily B (MDR/TAP)	gil147225187	0.02491	3	Peptide transporter activity

[a]Please refer to Supplemental Table 1, Supporting Information, for detailed listings of peptides, posterior error probability (PEP) for peptide identification, etc.
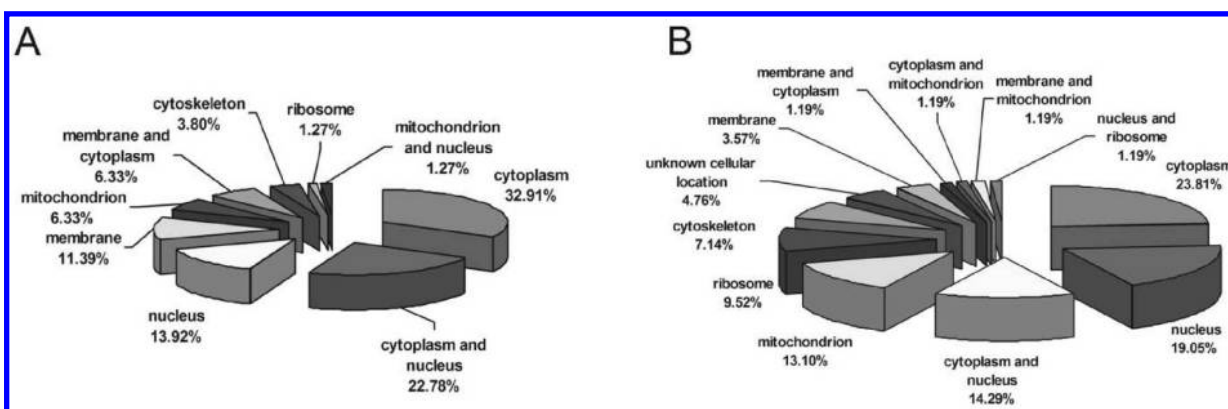
Figure 4. Subcellular locations of the proteins with differential expression (B ≤ 0.05) in PK-15 cells infected with PCV2. (A) Up-regulated proteins; (B) down-regulated proteins.

Western blotting results showed that the ratios of the three representative proteins between infected and uninfected cells were consistent with those obtained from SILAC.

DISCUSSION

Cellular processes such as gene expression, signaling pathways and morphology are altered by viral infection. High-throughput quantitative proteomics using SILAC is an ideal method to map such changes from the perspective of a cell, as it is suitable for unbiased comparison analysis.[32] To obtain more information about the virus-host interaction and the processes that lead to the onset of disease, the high-throughput quantitative proteomic approach using SILAC was utilized to investigate the differential proteomes of PK-15 cells in response to PCV2 infection. A total of 163 different proteins were identified as having altered abundances in PCV2-infected cells, including those involved in cell death, cellular growth and proliferation, and cellular assembly and organization.

Calpain-1, a calcium-dependent, nonlysosomal protease that exists widely in animal tissues,[33,34] was up-regulated approximately 28-fold in this study. Activated calpain cleaves a number of substrates, including cytoskeletal and membrane proteins, enzymes and transcription factors.[35,36] One of these substrates is the cytoskeletal element spectrin; spectrin contains SPTAN-1, which was down-regulated approximately 19-fold in our experiment (Table 1, Figure 7A). The other cytoskeletal substrate, desmin, was down-regulated approximately 21-fold (Table 1, Figure 7A). Spectrin is a major actin-binding cytoskeletal component and is a preferred substrate for calpain.[37] Calpain-mediated proteolysis of spectrin leads to the immediate production of breakdown products (BDPs). In previous studies, calpain activation was considered to be an early and causal event in the degeneration.[38] BDPs have been

found in stroke-type excitotoxicity, hypoxia/ischemia, vasospasm, epilepsy, toxin exposure, brain injury, kidney malfunction, and genetic defects.[38] Calpain activity is involved in a large number of physiological and pathological processes.[33] Because of their ability to remodel cytoskeletal anchorage complexes, calpains play major roles in the regulation of cell adhesion, migration and fusion, which are three key steps in myogenesis. Calcium-dependent proteolysis is also involved in cell cycle control. In muscle tissue, calpains intervene in the regeneration process. Another important class of calpain substrates is apoptosis-regulating factors, which may play a role in muscle cell death and consequently in muscle atrophy. Calpain proteolytic systems have been implicated in muscle wasting,[39] cardiac disease,[35] cancers,[40] and neurodegenerative diseases such as Huntington's disease[41] and Alzheimer's disease.[42−44] Calpain has also been reported to play a critical role in viral pathogenesis. Reports have shown that calpain activation by hepatitis C virus proteins inhibits the extrinsic apoptotic signaling pathway and increases the persistence of experimental viral infection in vivo.[45] Hepatitis B virus X protein up-regulates the expression of calpain small subunit 1 through NF-kB/p65, which can significantly enhance the migration ability of HepG2 cells.[46] HIV-1 transactivating factor (Tat) has been reported to activate calpain proteases via the ryanodine receptor to enhance surface dopamine transporter levels and promote synaptic dysfunction in HIV-associated neurologic disease.[47] Interestingly, ryanodine receptor 1 was up-regulated more than 7-fold in PCV2-infected PK-15 cells (Table 1). The symptoms caused by PCV2, including wasting, cardiac hypertrophy, myocarditis and congenital tremors (CT), in piglets are very similar to the human diseases linked to abnormalities in calpain expression or activation, which suggests that overexpression of calpain-1 in PCV2-infected PK-15 cells may play a critical role in PCV2 pathogenesis. On the other hand, calpain-2, which is another
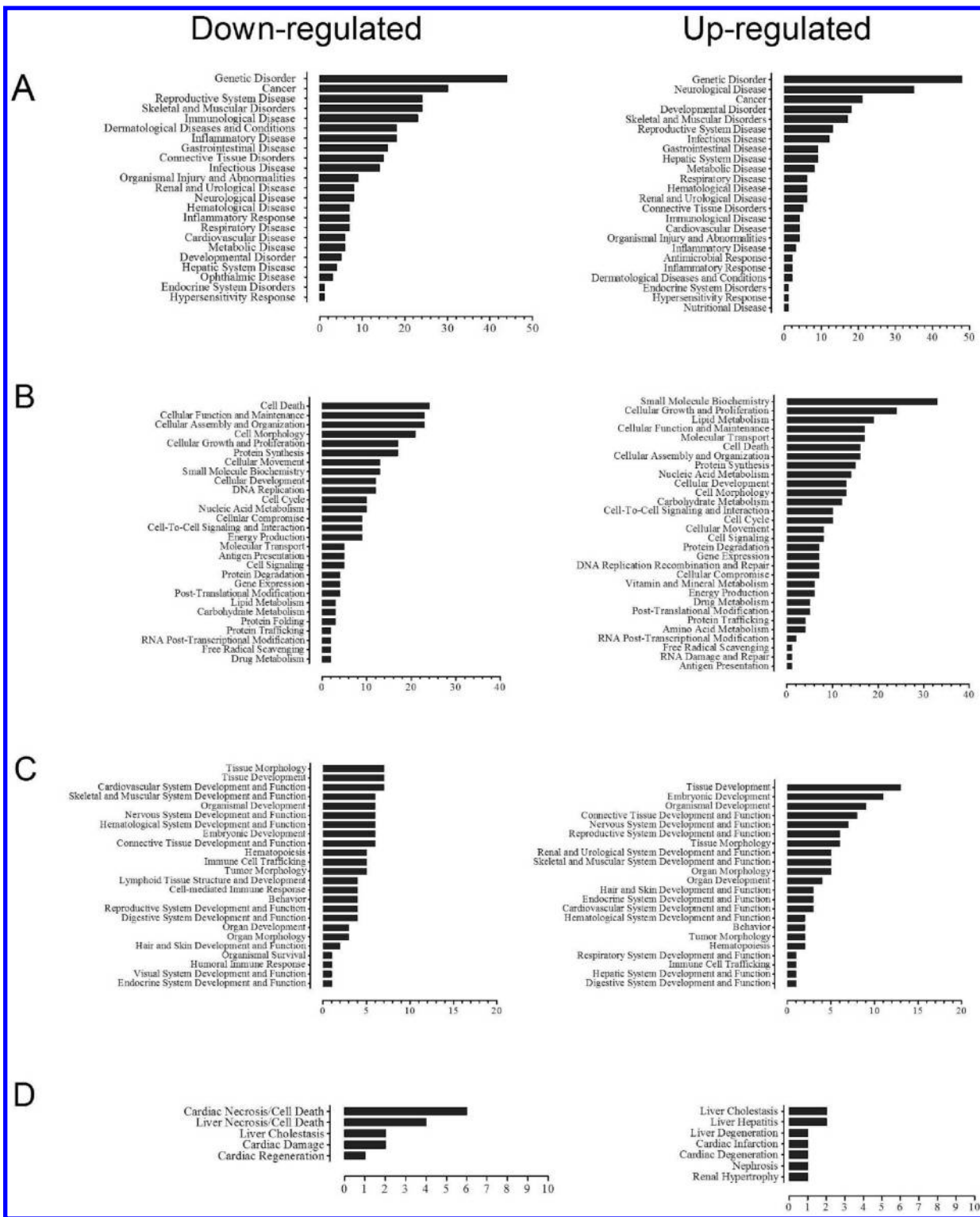
Figure 5. Functional characterization of up-regulated and down-regulated proteins. (A) Diseases and disorders; (B) molecular and cellular functions; (C) physiological system development and functions; (D) toxicity functions. More information is available in Supplementary Table 2, Supporting Information.

typical calpain isoform, was down-regulated approximately 5-fold (Supplementary Table 3, Supporting Information). Further large-scale studies are required to understand the roles and interrelation of calpain-1 and calpain-2 in PCV2-infected cells.

Recently, it was reported that a novel protein encoded by ORF3 is not essential for PCV2 replication in cultured PK-15

cells, but it plays a major role in virus-induced apoptosis by activating the caspase-8 and caspase-3 pathways.[11] In this study, apoptosis-related proteins, including caspase-3, caspase-7, Bax-alpha protein, and FADD-containing protein, were down-regulated more than 2-fold. This result may seem contradictory to the finding of PCV2-induced apoptosis; however, it should
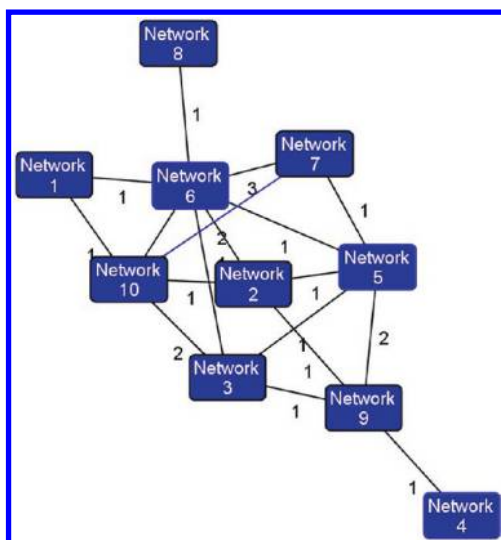
Figure 6. Overview of 10 specific functional networks, each of which contained 11 or more "focus" proteins (proteins that were significantly up- or down-regulated). Each box contains an arbitrary network number. The numbers between two networks represent the amount of overlapped proteins. More information is available in Supplementary Table 2, Supporting Information.

be noted that a number of proteins associated with apoptosis (both pro- and antiapoptotic proteins) are either activated or inactivated by calpains during apoptosis. Caspase-3, caspase-7, and Bax are calpain-cleaved substrates.[48−50] Calpains cleave and inactivate caspase-3, -7, and -9 in biochemical ex vivo apoptosis assays and during Ca^{2+} ionophore-induced apoptosis in vitro.[49] Contrarily, calpains apparently activate caspases in some experimental systems, including caspase-3 during cerebral hypoxia-ischemia[48] and caspase-7 in B cell apoptosis.[51] Another complexity is that members of the Bcl-2 family are cleaved by calpains: cleavage of Bax and Bid either generates novel pro-apoptotic fragments or inactivates their apoptotic func-tions.[11,50,52] The role of calpains in apoptosis is enigmatic, similar to their apparently different preferences for individual substrates among experimental systems, and appears to be highly dependent on the cell type and apoptotic stimulus.[36] In this study, calpain-cleaved products of apoptosis-related proteins might not be identified by LC−MS/MS, resulting in their apparent reduced expression levels. Whether the frag-ments produced by calpain cleavage possess apoptotic functions should be investigated. Although the activation of caspase-3 and caspase-8 has been demonstrated in PCV2-infected cells,[11] additional details of the apoptosis pathway need to be investigated. Collagen, a major structural protein in the flesh and connective tissues of mammals, was remarkably down-regulated in PCV2-infected cells. Degraded collagen has been reported to induce calpain-mediated apoptosis and destruction of the X-chromosome-linked inhibitor of apoptosis (xIAP) in human vascular smooth muscle cells.[53] These findings suggest that calpain is closely related to apoptosis and plays an important role in PCV2 pathogenesis.

It has been reported that the JNK1/2 and p38 MAPK pathways can be activated in PCV2-infected PK15 cells and that they play important roles in PCV2 replication.[17] In this study, 6 significantly down-regulated proteins (>2-fold) were mapped to the p38 MAPK pathway, including mitogen-activated protein kinase kinase (MAP2K4 or MKK4), FADD, H3F3A/H3F3B, STAT1, and HSPB1 (Supplementary Table 3, Supporting

Information). Whether the down-regulation of p38 MAPK pathway members is contradictory to its activation requires a comprehensive analysis. MKK4 is a critical component of the stress-activated MAP kinase signaling pathway. MKK4 has been reported to antagonize cardiomyocyte hypertrophy.[54] Mice with a cardiac-specific deletion of the mkk4 gene have an increased susceptibility to pathological cardiac hypertrophy.[54] The decreased expression of MKK4 seems to be consistent with the pathological response, including cardiac hypertrophy in PCV2-infected stillborn and nonviable neonatal piglets.

Many proteins that were significantly altered in abundance in virus-infected cells are related to intracellular substrate transport. Viral infection might selectively modify the expression profile of the cellular proteome in favor of viral propagation and assembly. The regulated import of molecules into the nucleus through nuclear pores is a vital event in eukaryotic cells. The nuclear import of proteins occurs through nuclear pore complexes (NPCs) and typically requires specific nuclear localization signals (NLSs). NLS-containing cargos are usually recognized by importin $\alpha−\beta$ heterodimers. Importin α serves as the NLS receptor, whereas importin β functions as an adapter that mediates binding to nucleoporins and trans-location of the trimeric complex into the nucleus.[55] Successful viral infections depend on the import of the viral genome and capsid proteins into the nucleus, where viral gene transcription, DNA replication, and virion maturation take place. Results from this study on the early phase of infection of cultured cells with PCV2 virions showed that karyopherin $\alpha2$ and importin 5, which belong to the cluster of importin α and β, respectively, were up-regulated. Karyopherin $\alpha2$, also named importin $\alpha1$, may interact with viral proteins to enhance the efficiency of the transport of these proteins into host cell nuclei. The adaptive mutations in polymerase subunit PB2 and NP of avian influenza virus improves the binding of these proteins to importin $\alpha1$ in mammalian cells, which is paralleled by the increased transport of PB2 and NP into the nucleus.[56] This conclusion was confirmed, promoting viral infection, for the Epstein−Barr virus (EBV),[57] Herpesvirus saimiri (HVS),[58] human papillomaviruses (HPVs)[59] and HIV-1.[60] Importin 5 is an import factor that plays a biological role in the nuclear import and assembly of the influenza virus RNA polymerase complex.[61]

Cytoskeletal changes are associated with transcellular membrane trafficking, which is facilitated for viral replication. Together, β-tubulin (Supplementary Table 3, Supporting Information) and α-tubulin (Table 1) participate in the formation of microtubules, the integrity of which is essential for the segregation of chromosomes during cell division, the maintenance of cell shape, and the intracellular trafficking of macromolecules and organelles. With regard to β-tubulin, there are several reports showing that viruses may require micro-tubule components for RNA synthesis.[62] α-Tubulin was identified as being overexpressed when it interacts with Rep of PCV2 through colocalization and coimmunoprecipitation ananlyses,[20] while β-tubulin expression was approximately 5-fold down-regulated. Changes in β-tubulin and vimentin levels have been detected in SARS-CoV[22] and infectious bursal disease virus (IBDV).[63] However, most of the cytoskeletal altera-tions detected in PCV2-infected cells were down-regulated in response to viral infection in this study (Table 1). Some cytoskeletal members may be degraded by calpain-1 that overexpressed in PCV2-infected cells, but further investigations are required about the consistent reduction of many cytoskeletal
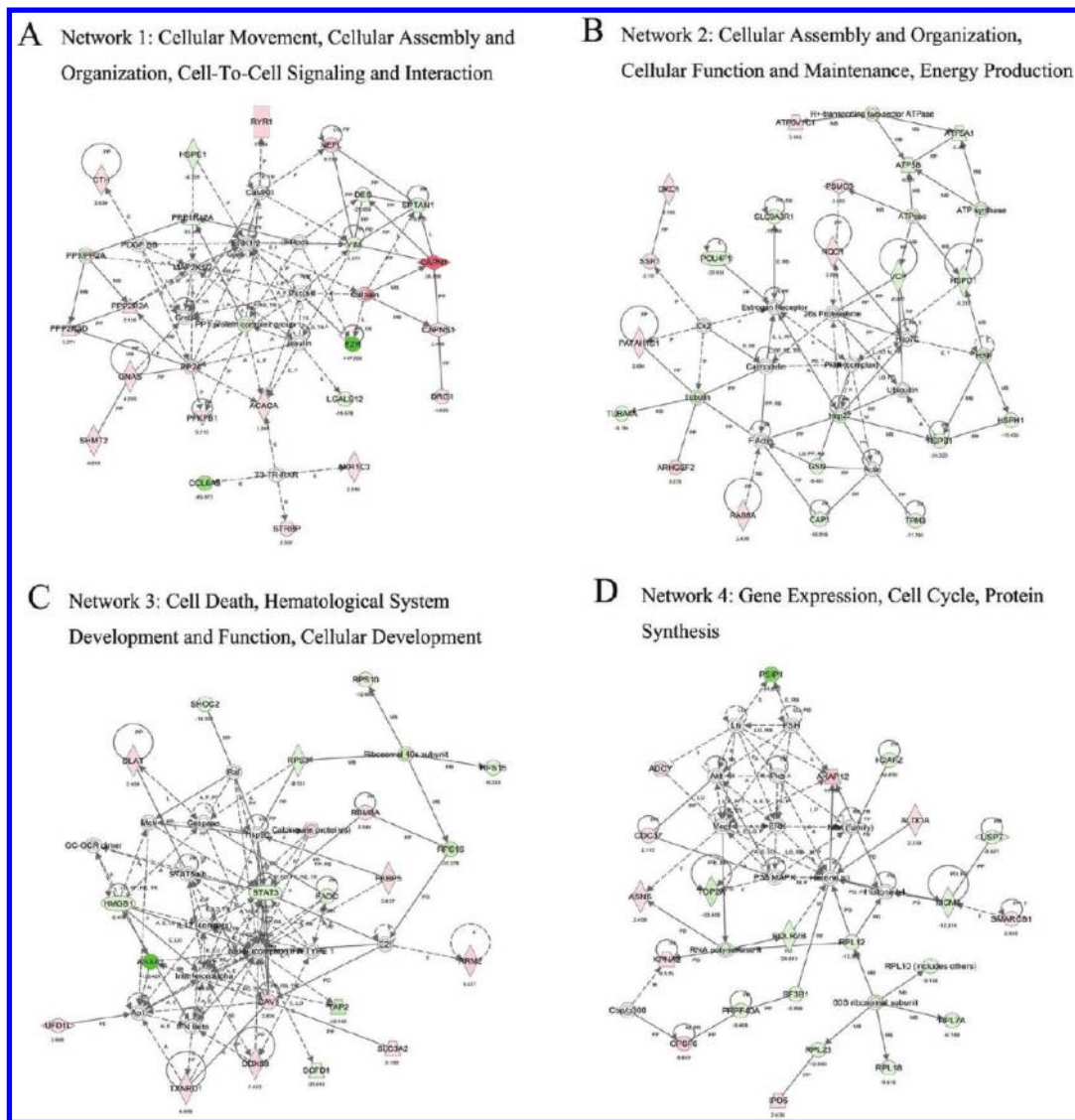
Figure 7. Ingenuity Pathway Analysis of proteins that were significantly altered in PCV2-infected PK-15 cells. Red, up-regulated proteins; green, significantly down-regulated proteins; white, proteins known to be in the network but were not identified in our study. The color depth indicates the magnitude of the change in protein expression level. The numbers represent value of SILAC ratios). The shapes are indicative of the molecular class (i.e., protein family) (see Supplementary Figure 1 for legend, Supporting Information). Lines connecting the molecules indicate molecular relationships. Dashed lines indicate indirect interactions, and solid lines indicate direct interactions. The arrow styles indicate specific molecular relationships and the directionality of the interaction.
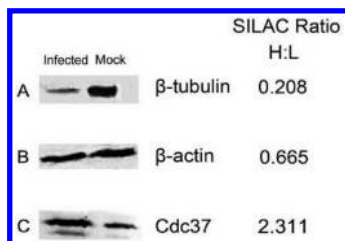
Figure 8. Representative protein quantitative confirmation with Western blotting. (A) β-Tubulin; (B) β-actin; (C) Cdc37. SILAC ratios (H:L) are shown on the right side.

components. We speculate that the vimentin and β-tubulin networks collapse and disperse in host cells, leading to an unstable cytoskeletal structure, so cytoskeletal disruption may be a critical mechanism of viral particle release from infected cells.[64−66] Furthermore, proteolytic cleavage of vimentin during

HCV (hepatitis C virus) infection has been reported as being necessary for productive infection.[67]

The heat shock response or stress response is the most highly conserved cellular response in all species; these responses antagonize external stress. Heat shock proteins (HSPs) have been shown to participate in antigen presentation and intracellular trafficking and apoptosis and act as molecular chaperones by helping nascent polypeptides assume their proper conformations.[88] The results of the present study demonstrated that several proteins concerning HSPs had reduced levels (>2-fold change), including hsp90, hsp40, hsp60, hsp10 and hsp105 (Supplementary Table 1 and Table 3, Supporting Information). Currently, several members of the HSP family were found to be expressed on the surfaces of cells and have been shown to stimulate immune effector cells directly or play crucial roles in antigen cross-priming by acting as shuttle molecules for exogenous antigens and as direct stimulants of T cells by prompting APC cytokine secretion.[69]

HSPs appear to be involved in innate immune responses since the emergence of phagocytes in early multicellular organisms and have been commandeered for adaptive immune responses with the advent of immune specificity.[70] HSP90 is important for the stimulation of $\gamma\delta$-T cells and serves as an immune sentinel trigger during acute virus infection or as an aid in the generation of EBV-specific T cells during AIM convalescence.[69] Hsp60 has direct modulatory effects on inflammatory cells, which can activate monocytes and granulocytes to produce inflammatory cytokines, tumor necrosis factor a (α-TNF), interleukin 12 (IL-12) and IL-6.[71] This conclusion follows directly from data suggesting that PCV2 infection weakens the expression levels of heat shock proteins to handicap their ability to induce a protective immune response when immunocytes are confronted with foreign entities. Suppression of hsps obstructs antigen presentation, which activates the innate and adaptive immune systems to initiate an acute response to viral infection. These properties of heat shock proteins also allow them to be used in the immunotherapy of infections in novel ways, which could lead to a greater understanding of how PCV2 modulates the immune response of the host and why this virus induces immunosuppression in PMWS-affected pigs.

In summary, the proteomic alterations of PCV2-infected PK-15 cells were characterized using SILAC combined with LC−MS/MS. A comprehensive network of protein regulation in PCV2-infected PK-15 cells was constructed in this study. Although many significantly regulated proteins and pathways are closely related to the symptoms or pathological responses of PCV2 infection, further functional investigations should be carried out to facilitate our understanding of the pathogenic mechanisms and molecular responses of host cells to PCV2 infection. Further work may provide the identification of therapeutic targets or lead to the development of new methods of preventing PCV2 infection.

ASSOCIATED CONTENT

Ⓢ Supporting Information

Information for each significantly changed proteins identified and data of MS/MS analyses of single peptide-based proteins with altered expression. Functional characterization of up- and down-regulated proteins in PCV2-infected cells, networks and pathways analysis, and the legend of IPA. This material is available free of charge via the Internet at http://pubs.acs.org.

AUTHOR INFORMATION

Corresponding Author

*Dr. Ming Liao, College of Veterinary Medicine, South China Agricultural University, Guangzhou 510642, China. E-mail: mliao@scau.edu.cn. Tel/Fax: 0086-20-85280240.

Author Contributions

§These authors contributed equally to this work.

ACKNOWLEDGMENTS

ABBREVIATIONS

AIM, acute infectious mononucleosis; CID, collision induced dissociation; FADD, FAS-associating death domain-containing protein; FDR, false discovery rate; FITC, fluorescein isothocyanate; HSP, heat shock protein; PEP, posterior error probability; PMWS, postweaning multisystemic wasting syndrome; SATA, signal transducers and activators of transcription protein; SDS-PAGE, sodium dodecyl sulfate polyacrylamide gel electrophoresis

REFERENCES

(1) Cheng, C. C.; Lee, Y. F.; Lin, N. N.; Wu, C. L.; Tung, K. C.; Chiu, Y. T. Bronchiolitis obliterans organizing pneumonia in Swine associated with porcine circovirus type 2 infection. *J. Biomed. Biotechnol.* **2011**, *2011*, 245728.

(2) Lin, C. M.; Jeng, C. R.; Hsiao, S. H.; Liu, J. P.; Chang, C. C.; Chiou, M. T.; Tsai, Y. C.; Chia, M. Y.; Pang, V. F. Immunopathological characterization of porcine circovirus type 2 infection-associated follicular changes in inguinal lymph nodes using high-throughput tissue microarray. *Vet. Microbiol.* **2011**, *149* (1−2), 72−84.

(3) Madec, F.; Rose, N.; Grasland, B.; Cariolet, R.; Jestin, A. Postweaning multisystemic wasting syndrome and other PCV2-related problems in pigs: a 12-year experience. *Transbound Emerg. Dis.* **2008**, *55* (7), 273−83.

(4) Madson, D. M.; Patterson, A. R.; Ramamoorthy, S.; Pal, N.; Meng, X. J.; Opriessnig, T. Reproductive failure experimentally induced in sows via artificial insemination with semen spiked with porcine circovirus type 2. *Vet. Pathol.* **2009**, *46* (4), 707−16.

(5) Darwich, L.; Segales, J.; Mateu, E. Pathogenesis of postweaning multisystemic wasting syndrome caused by Porcine circovirus 2: An immune riddle. *Arch. Virol.* **2004**, *149* (5), 857−74.

(6) Crowther, R. A.; Berriman, J. A.; Curran, W. L.; Allan, G. M.; Todd, D. Comparison of the structures of three circoviruses: chicken anemia virus, porcine circovirus type 2, and beak and feather disease virus. *J. Virol.* **2003**, *77* (24), 13036−41.

(7) Hamel, A. L.; Lin, L. L.; Nayar, G. P. Nucleotide sequence of porcine circovirus associated with postweaning multisystemic wasting syndrome in pigs. *J. Virol.* **1998**, *72* (6), 5262−7.

(8) Mankertz, A.; Persson, F.; Mankertz, J.; Blaess, G.; Buhk, H. J. Mapping and characterization of the origin of DNA replication of porcine circovirus. *J. Virol.* **1997**, *71* (3), 2562−6.

(9) Nawagitgul, P.; Morozov, I.; Bolin, S. R.; Harms, P. A.; Sorden, S. D.; Paul, P. S. Open reading frame 2 of porcine circovirus type 2 encodes a major capsid protein. *J. Gen. Virol.* **2000**, *81* (Pt 9), 2281−7.

(10) Fort, M.; Sibila, M.; Nofrarias, M.; Perez-Martin, E.; Olvera, A.; Mateu, E.; Segales, J. Porcine circovirus type 2 (PCV2) Cap and Rep proteins are involved in the development of cell-mediated immunity upon PCV2 infection. *Vet. Immunol. Immunopathol.* **2010**, *137* (3−4), 226−34.

(11) Liu, J.; Chen, I.; Kwang, J. Characterization of a previously unidentified viral protein in porcine circovirus type 2-infected cells and its role in virus-induced apoptosis. *J. Virol.* **2005**, *79* (13), 8262−74.

(12) Balmelli, C.; Steiner, E.; Moulin, H.; Peduto, N.; Herrmann, B.; Summerfield, A.; McCullough, K. Porcine circovirus type 2 DNA influences cytoskeleton rearrangements in plasmacytoid and monocyte-derived dendritic cells. *Immunology* **2011**, *132* (1), 57−65.

(13) Chae, J. S.; Choi, K. S. Proinflammatory cytokine expression in the lung of pigs with porcine circovirus type 2-associated respiratory disease. *Res. Vet. Sci.* **2011**, *90* (2), 321−3.

(14) Tsai, Y. C.; Jeng, C. R.; Hsiao, S. H.; Chang, H. W.; Liu, J. J.; Chang, C. C.; Lin, C. M.; Chia, M. Y.; Pang, V. F. Porcine circovirus type 2 (PCV2) induces cell proliferation, fusion, and chemokine expression in swine monocytic cells in vitro. *Vet. Res.* **2010**, *41* (5), 60.

(15) Hasslung, F. C.; Berg, M.; Allan, G. M.; Meehan, B. M.; McNeilly, F.; Fossum, C. Identification of a sequence from the genome of porcine circovirus type 2 with an inhibitory effect on IFN-alpha production by porcine PBMCs. *J. Gen. Virol.* **2003**, *84* (Pt 11), 2937−45.

(16) Karuppannan, A. K.; Liu, S.; Jia, Q.; Selvaraj, M.; Kwang, J. Porcine circovirus type 2 ORF3 protein competes with p53 in binding to Pirh2 and mediates the deregulation of p53 homeostasis. *Virology* **2010**, *398* (1), 1−11.

(17) Wei, L.; Zhu, Z.; Wang, J.; Liu, J. JNK and p38 mitogen-activated protein kinase pathways contribute to porcine circovirus type 2 infection. *J. Virol.* **2009**, *83* (12), 6039−47.

(18) Finsterbusch, T.; Steinfeldt, T.; Doberstein, K.; Rodner, C.; Mankertz, A. Interaction of the replication proteins and the capsid protein of porcine circovirus type 1 and 2 with host proteins. *Virology* **2009**, *386* (1), 122−31.

(19) Timmusk, S.; Fossum, C.; Berg, M. Porcine circovirus type 2 replicase binds the capsid protein and an intermediate filament-like protein. *J. Gen. Virol.* **2006**, *87* (Pt 11), 3215−23.

(20) Zhang, X.; Zhou, J.; Wu, Y.; Zheng, X.; Ma, G.; Wang, Z.; Jin, Y.; He, J.; Yan, Y. Differential proteome analysis of host cells infected with porcine circovirus type 2. *J. Proteome Res.* **2009**, *8* (11), 5111−9.

(21) Emmott, E.; Wise, H.; Loucaides, E. M.; Matthews, D. A.; Digard, P.; Hiscox, J. A. Quantitative proteomics using SILAC coupled to LC−MS/MS reveals changes in the nucleolar proteome in influenza A virus-infected cells. *J. Proteome Res.* **2010**, *9* (10), 5335−45.

(22) Jiang, X. S.; Tang, L. Y.; Dai, J.; Zhou, H.; Li, S. J.; Xia, Q. C.; Wu, J. R.; Zeng, R. Quantitative analysis of severe acute respiratory syndrome (SARS)-associated coronavirus-infected cells using proteomic approaches: implications for cellular responses to virus infection. *Mol. Cell. Proteomics* **2005**, *4* (7), 902−13.

(23) Skiba, M.; Glowinski, F.; Koczan, D.; Mettenleiter, T. C.; Karger, A. Gene expression profiling of Pseudorabies virus (PrV) infected bovine cells by combination of transcript analysis and quantitative proteomic techniques. *Vet. Microbiol.* **2010**, *143* (1), 14−20.

(24) Emmott, E.; Rodgers, M. A.; Macdonald, A.; McCrory, S.; Ajuh, P.; Hiscox, J. A. Quantitative proteomics using stable isotope labeling with amino acids in cell culture reveals changes in the cytoplasmic, nuclear, and nucleolar proteomes in Vero cells infected with the coronavirus infectious bronchitis virus. *Mol. Cell. Proteomics* **2010**, *9* (9), 1920−36.

(25) Lam, Y. W.; Evans, V. C.; Heesom, K. J.; Lamond, A. I.; Matthews, D. A. Proteomics analysis of the nucleolus in adenovirus-infected cells. *Mol. Cell. Proteomics* **2010**, *9* (1), 117−30.

(26) Mannova, P.; Fang, R.; Wang, H.; Deng, B.; McIntosh, M. W.; Hanash, S. M.; Beretta, L. Modification of host lipid raft proteome upon hepatitis C virus replication. *Mol. Cell. Proteomics* **2006**, *5* (12), 2319−25.

(27) Munday, D. C.; Emmott, E.; Surtees, R.; Lardeau, C. H.; Wu, W.; Duprex, W. P.; Dove, B. K.; Barr, J. N.; Hiscox, J. A. Quantitative proteomic analysis of A549 cells infected with human respiratory syncytial virus. *Mol. Cell. Proteomics* **2010**, *9* (11), 2438−59.

(28) Pathak, S.; De Souza, G. A.; Salte, T.; Wiker, H. G.; Asjo, B. HIV induces both a down-regulation of IRAK-4 that impairs TLR signalling and an up-regulation of the antibiotic peptide dermcidin in monocytic cells. *Scand. J. Immunol.* **2009**, *70* (3), 264−76.

(29) Yan, G. R.; Xu, S. H.; Tan, Z. L.; Liu, L.; He, Q. Y. Global identification of miR-373-regulated genes in breast cancer by quantitative proteomics. *Proteomics* **2011**, *11* (5), 912−20.

(30) Cox, J.; Mann, M. MaxQuant enables high peptide identification rates, individualized p.p.b.-range mass accuracies and proteome-wide protein quantification. *Nat. Biotechnol.* **2008**, *26* (12), 1367−72.

(31) Sun, J.; Jiang, Y.; Shi, Z.; Yan, Y.; Guo, H.; He, F.; Tu, C. Proteomic alteration of PK-15 cells after infection by classical swine fever virus. *J. Proteome Res.* **2008**, *7* (12), 5263−9.

(32) Mann, M. Functional and quantitative proteomics using SILAC. *Nat. Rev. Mol. Cell. Biol.* **2006**, *7* (12), 952−8.

(33) Croall, D. E.; Ersfeld, K. The calpains: modular designs and functional diversity. *Genome Biol.* **2007**, *8* (6), 218.

(34) Melloni, E.; Pontremoli, S. The calpains. *Trends Neurosci.* **1989**, *12* (11), 438−44.

(35) Perrin, C.; Vergely, C.; Rochette, L. [Calpains and cardiac diseases]. *Ann. Cardiol. Angeiol. (Paris)* **2004**, *53* (5), 259−66.

(36) Goll, D. E.; Thompson, V. F.; Li, H.; Wei, W.; Cong, J. The calpain system. *Physiol. Rev.* **2003**, *83* (3), 731−801.

(37) Boivin, P.; Galand, C.; Dhermy, D. In vitro digestion of spectrin, protein 4.1 and ankyrin by erythrocyte calcium dependent neutral protease (calpain I). *Int. J. Biochem.* **1990**, *22* (12), 1479−89.

(38) Vanderklish, P. W.; Bahr, B. A. The pathogenic activation of calpain: a marker and mediator of cellular toxicity and disease states. *Int. J. Exp. Pathol.* **2000**, *81* (5), 323−39.

(39) Bartoli, M.; Richard, I. Calpains in muscle wasting. *Int. J. Biochem. Cell Biol.* **2005**, *37* (10), 2115−33.

(40) Guicciardi, M. E.; Gores, G. J. Calpains can do it alone: implications for cancer therapy. *Cancer Biol. Ther.* **2003**, *2* (2), 153−4.

(41) Gafni, J.; Ellerby, L. M. Calpain activation in Huntington's disease. *J. Neurosci.* **2002**, *22* (12), 4842−9.

(42) Garg, S.; Timm, T.; Mandelkow, E. M.; Mandelkow, E.; Wang, Y. Cleavage of Tau by calpain in Alzheimer's disease: the quest for the toxic 17 kD fragment. *Neurobiol. Aging* **2011**, *32* (1), 1−14.

(43) Zatz, M.; Starling, A. Calpains and disease. *N. Engl. J. Med.* **2005**, *352* (23), 2413−23.

(44) Adamec, E.; Mohan, P.; Vonsattel, J. P.; Nixon, R. A. Calpain activation in neurodegenerative diseases: confocal immuno-fluorescence study with antibodies specifically recognizing the active form of calpain 2. *Acta Neuropathol.* **2002**, *104* (1), 92−104.

(45) Simonin, Y.; Disson, O.; Lerat, H.; Antoine, E.; Biname, F.; Rosenberg, A. R.; Desagher, S.; Lassus, P.; Bioulac-Sage, P.; Hibner, U. Calpain activation by hepatitis C virus proteins inhibits the extrinsic apoptotic signaling pathway. *Hepatology* **2009**, *50* (5), 1370−9.

(46) Zhang, F.; Wang, Q.; Ye, L.; Feng, Y.; Zhang, X. Hepatitis B virus X protein upregulates expression of calpain small subunit 1 via nuclear factor-kappaB/p65 in hepatoma cells. *J. Med. Virol.* **2010**, *82* (6), 920−8.

(47) Perry, S. W.; Barbieri, J.; Tong, N.; Polesskaya, O.; Pudasaini, S.; Stout, A.; Lu, R.; Kiebala, M.; Maggirwar, S. B.; Gelbard, H. A. Human immunodeficiency virus-1 Tat activates calpain proteases via the ryanodine receptor to enhance surface dopamine transporter levels and increase transporter-specific uptake and Vmax. *J. Neurosci.* **2010**, *30* (42), 14153−64.

(48) Blomgren, K.; Zhu, C.; Wang, X.; Karlsson, J. O.; Leverin, A. L.; Bahr, B. A.; Mallard, C.; Hagberg, H. Synergistic activation of caspase-3 by m-calpain after neonatal hypoxia-ischemia: a mechanism of "pathological apoptosis"? *J. Biol. Chem.* **2001**, *276* (13), 10191−8.

(49) Chua, B. T.; Guo, K.; Li, P. Direct cleavage by the calcium-activated protease calpain can lead to inactivation of caspases. *J. Biol. Chem.* **2000**, *275* (7), 5131−5.

(50) Wood, D. E.; Thomas, A.; Devi, L. A.; Berman, Y.; Beavis, R. C.; Reed, J. C.; Newcomb, E. W. Bax cleavage is mediated by calpain during drug-induced apoptosis. *Oncogene* **1998**, *17* (9), 1069−78.

(51) Ruiz-Vela, A.; Gonzalez, D. B. G.; Martinez-A, C. Implication of calpain in caspase activation during B cell clonal deletion. *EMBO J.* **1999**, *18* (18), 4988−98.

(52) Nakagawa, T.; Yuan, J. Cross-talk between two cysteine protease families. Activation of caspase-12 by calpain in apoptosis. *J. Cell Biol.* **2000**, *150* (4), 887−94.

(53) von Wnuck, L. K.; Keul, P.; Lucke, S.; Heusch, G.; Wohlschlaeger, J.; Baba, H. A.; Levkau, B. Degraded collagen induces calpain-mediated apoptosis and destruction of the X-chromosome-linked inhibitor of apoptosis (xIAP) in human vascular smooth muscle cells. *Cardiovasc. Res.* **2006**, *69* (3), 697−705.

(54) Liu, W.; Zi, M.; Jin, J.; Prehar, S.; Oceandy, D.; Kimura, T. E.; Lei, M.; Neyses, L.; Weston, A. H.; Cartwright, E. J.; Wang, X. Cardiac-specific deletion of mkk4 reveals its role in pathological hypertrophic remodeling but not in physiological cardiac growth. *Circ. Res.* **2009**, *104* (7), 905−14.

(55) Ma, J.; Cao, X. Regulation of Stat3 nuclear import by importin alpha5 and importin alpha7 via two different functional sequence elements. *Cell Signal.* **2006**, *18* (8), 1117−26.

(56) Gabriel, G.; Herwig, A.; Klenk, H. D. Interaction of polymerase subunit PB2 and NP with importin alpha1 is a determinant of host range of influenza A virus. *PLoS Pathog.* **2008**, *4* (2), e11.

(57) Fischer, N.; Kremmer, E.; Lautscham, G.; Mueller-Lantzsch, N.; Grasser, F. A. Epstein-Barr virus nuclear antigen 1 forms a complex with the nuclear transporter karyopherin alpha2. *J. Biol. Chem.* **1997**, *272* (7), 3999−4005.

(58) Goodwin, D. J.; Whitehouse, A. A gamma-2 herpesvirus nucleocytoplasmic shuttle protein interacts with importin alpha 1 and alpha 5. *J. Biol. Chem.* **2001**, *276* (23), 19905−12.

(59) Merle, E.; Rose, R. C.; LeRoux, L.; Moroianu, J. Nuclear import of HPV11 L1 capsid protein is mediated by karyopherin alpha2beta1 heterodimers. *J. Cell Biochem.* **1999**, *74* (4), 628−37.

(60) Vodicka, M. A.; Koepp, D. M.; Silver, P. A.; Emerman, M. HIV-1 Vpr interacts with the nuclear transport pathway to promote macrophage infection. *Genes Dev.* **1998**, *12* (2), 175−85.

(61) Deng, T.; Engelhardt, O. G.; Thomas, B.; Akoulitchev, A. V.; Brownlee, G. G.; Fodor, E. Role of ran binding protein 5 in nuclear import and assembly of the influenza virus RNA polymerase complex. *J. Virol.* **2006**, *80* (24), 11911−9.

(62) Chongsatja, P. O.; Bourchookarn, A.; Lo, C. F.; Thongboonkerd, V.; Krittanai, C. Proteomic analysis of differentially expressed proteins in Penaeus vannamei hemocytes upon Taura syndrome virus infection. *Proteomics* **2007**, *7* (19), 3592−601.

(63) Zheng, X.; Hong, L.; Shi, L.; Guo, J.; Sun, Z.; Zhou, J. Proteomics analysis of host cells infected with infectious bursal disease virus. *Mol. Cell. Proteomics* **2008**, *7* (3), 612−25.

(64) Pocernich, C. B.; Boyd-Kimball, D.; Poon, H. F.; Thongboonkerd, V.; Lynn, B. C.; Klein, J. B.; Calebrese, V.; Nath, A.; Butterfield, D. A. Proteomics analysis of human astrocytes expressing the HIV protein Tat. *Brain Res. Mol. Brain Res.* **2005**, *133*, 2.

(65) Chen, W.; Gao, N.; Wang, J. L.; Tian, Y. P.; Chen, Z. T.; An, J. Vimentin is required for dengue virus serotype 2 infection but microtubules are not necessary for this process. *Arch. Virol.* **2008**, *153* (9), 1777−81.

(66) Fang, M.; Nie, Y.; Theilmann, D. A. AcMNPV EXON0 (AC141) which is required for the efficient egress of budded virus nucleocapsids interacts with beta-tubulin. *Virology* **2009**, *385* (2), 496−504.

(67) Nitahara-Kasahara, Y.; Fukasawa, M.; Shinkai-Ouchi, F.; Sato, S.; Suzuki, T.; Murakami, K.; Wakita, T.; Hanada, K.; Miyamura, T.; Nishijima, M. Cellular vimentin content regulates the protein level of hepatitis C virus core protein and the hepatitis C virus production in cultured cells. *Virology* **2009**, *383* (2), 319−27.

(68) Khar, A.; Ali, A. M.; Pardhasaradhi, B. V.; Varalakshmi, C. H.; Anjum, R.; Kumari, A. L. Induction of stress response renders human tumor cell lines resistant to curcumin-mediated apoptosis: role of reactive oxygen intermediates. *Cell Stress Chaperones* **2001**, *6* (4), 368−76.

(69) Kotsiopriftis, M.; Tanner, J. E.; Alfieri, C. Heat shock protein 90 expression in Epstein-Barr virus-infected B cells promotes gammadelta T-cell proliferation in vitro. *J. Virol.* **2005**, *79* (11), 7255−61.

(70) Srivastava, P. Interaction of heat shock proteins with peptides and antigen presenting cells: chaperoning of the innate and adaptive immune responses. *Annu. Rev. Immunol.* **2002**, *20*, 395−425.

(71) Wells, A. D.; Malkovsky, M. Heat shock proteins, tumor immunogenicity and antigen presentation: an integrated view. *Immunol. Today* **2000**, *21* (3), 129−32.